Contents lists available at SciVerse ScienceDirect

CIRP Annals Manufacturing Technology

Journal homepage: www.elsevier.com/locate/cirp

An Experimental Methodology to Improve the Robotic Drilling of Aluminium Alloys

François Ducobu (2)[a], Thomas Beuscart[a,b], Valentin Dambly[a], Edouard Rivière-Lorphèvre[a], Gorka Ortiz-de-Zarate[b], Pedro-José Arrazola (1)[b]

[a] *Machine Design and Production Engineering Lab, Research Institute for Science and Material Engineering, UMONS, Belgium*
[b] *Mondragon Unibertsitatea, Faculty of Engineering, Department of Mechanics and Industrial Production, Loramendi 4, Arrasate-Mondragón 20500, Spain*

In aeronautics, mastering the drilling process is crucial to meet strict quality standards. While robots provide a cost-effective solution for drilling large, complex parts, challenges arise in metallic materials due to their low stiffness. This study establishes a systematic experimental method to improve hole quality during robotic drilling of aluminium alloys. Holes were drilled in plates in four positions and 64 postures using a 6 mm tool to analyse their influence on a new defect index. A static deflection compensation method was developed to improve hole quality, addressing static deflection issues narrowing the gap between robotic drilling and CNC machining.

Keywords: Drilling, Robot, Aluminium

1. Introduction

The flexibility of 6-axis robots makes them attractive for machining (e.g., trimming, drilling and countersinking) and finishing large, complex parts. However, they are mainly used for materials with low specific energy (e.g., composites, wood) [1]. For metals, the combination of high cutting forces and low stiffness results in significant defects: vibrations, chatter, dimensional inaccuracies, geometric errors, and poor surface finishes [2]. In drilling, compliance-induced defects include entry eccentricities, positional errors exceeding 0.5 mm, axial misalignments, poor surface finishes (*Ra* > 6.4 µm), and tool breakage [3].

In aerospace, strict quality standards amplify these challenges with tolerances on hole diameter deviations (below 0.08 mm), off-axis deviations (±0.5°), and positional errors (≤0.5 mm) [4]. Combined with the complexity of large, thin-walled structures [5], these stringent requirements make robotic drilling particularly challenging. Addressing these issues has led to the development of various strategies to mitigate the defects caused by high robotic compliance. These strategies fall into three approaches. (i) Hardware-based solutions involve modifications to the end-effector or tool system [6], such as integrating a pressure foot or using vibration-assisted systems [7]. For example, Bu et al. [8] showed that applying controlled pressure (500-1000 N) to the workpiece improves rigidity and hole quality. However, these methods often entail high setup costs due to hardware additions and risks, especially for thin-walled plates prone to deformation. (ii) Posture optimization methods focus on adjusting robotic posture to minimize compliance during machining. Bu et al. [8] recommended reducing axial compliance to lower entry eccentricities, while Lee et al. [9] employed deformation energy models to optimize compliance ellipsoids. These approaches exploit the robot's geometry to enhance performance without the need for external devices. (iii) Trajectory compensation techniques actively correct positioning errors caused by compliance or temperature effects [10]. In-situ systems like laser trackers have achieved final positional accuracy of ±0.07 mm in composite drilling [11]. However, these systems often require additional hardware, extensive calibration, and significant setup time, limiting their industrial feasibility.

Although existing strategies effectively mitigate robotic defects, they often involve high costs, complex setups, and reliance on additional hardware. It is therefore essential to develop methodologies that use only the robot's existing axes, eliminating the need for additional equipment or external actuation, thereby reducing implementation complexity and cost while maintaining operational flexibility. Moreover, the direct influence of robotic compliance on hole quality remains understudied, hindering the development of reliable criteria for predicting and mitigating defects during robotic drilling.

This study proposed a phenomenological experimental approach to systematically improve hole quality during robotic drilling of aluminium alloys by combining posture optimization (strategy (ii)) and trajectory compensation (strategy (iii)) without the need for any external devices (such as pressure foot or end-effector). Standardized measurements of diameter, roundness, cylindricity, and axial deviation were used to establish a hole defect criterion that directly correlates robotic compliance with hole quality. Additionally, by integrating compliance mapping with experimental cutting force measurements, strategies were developed to compensate for compliance-induced quasi-static defects. Robotic drilling results were benchmarked against CNC-drilled holes under varying cutting conditions to validate the proposed approach. This method enhances the understanding of compliance effects and demonstrates the industrial feasibility of achieving high-quality robotic drilling without additional hardware or complex setups.

2. Methodology

2.1. Experimental setup and measurements

The experimental drilling tests were conducted in a robotic cell equipped with a Stäubli TX200 6-axis robot, offering a 2.65 m range and a 130 kg maximum load capacity, fitted with a Teknomotor 7.8 kW machining spindle (Fig. 1(a)). A rigid fixture setup, including a hydraulic vise and clamping system including a support with a precise imprint, ensured stability. For comparison, a Lagun GVC 1000-HS 3-axis CNC machine was also used (Fig. 1(b)).

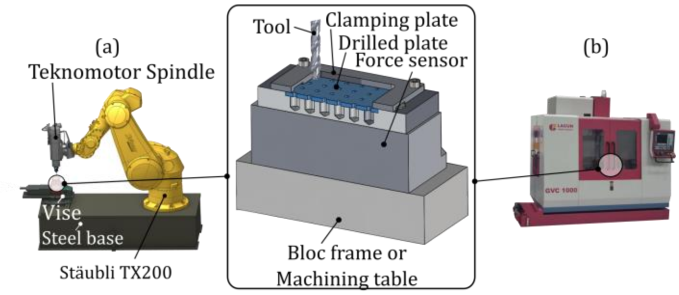

Figure 1. Experimental setup used for Robotic (a) and CNC drilling (b) of Al 6082-T6

The tests used 5 mm thick 6082-T6 aluminium samples, cold-cut by water jet. Cutting forces were measured with Kistler 9257B (robot) and Kistler 9113AA (CNC Machine). Tool integrity and optical analyses employed a Dino-Lite AM7013ZT microscope. Surface roughness and 1D profilometry were assessed with a Diavite DH-6 profilometer. Dimensional and geometric evaluations were conducted using a Mitutoyo Crysta-Apex V CMM with a Renishaw A-5003-0050 stylus. Each hole was measured with 216 data points (18 points per plane at 12 depth levels) to generate a point cloud for comprehensive hole quality analysis. The measurement planes at the hole's entry, middle, and exit are designated by the letters *e*, *m*, and *s*, corresponding to depth levels 1 (z=0 mm), 6 (z=-2.5 mm), and 12 (z=-5mm), respectively.

The tools were selected in a previous research work [3], which demonstrated that universal tool geometries with features reducing cutting forces are essential for high-quality robotic drilling of Al 6082-T6. The main characteristics and cutting conditions are detailed in Table 1. An initial set of tests (i) was performed exclusively on the robot, following the methodology outlined in *section 2.3*, using nominal cutting conditions based on the literature [3]. These conditions were selected to avoid undesirable dynamic effects such as natural modes and to ensure hole quality while balancing production efficiency (high feed rate) and the robot's maximum allowable load (approximately 1000 N). Additionally, a second set of tests (ii) was conducted on both the robot and the CNC machine to assess varying cutting conditions across the range specified in Table 1. All the tests were carried out in dry conditions and with unworn cutting tools.

Table 1. Tools and cutting conditions

Tool		
Reference	Holex 122771	
Diameter φ_i [mm]	6	
Helix angle [°]	33	
Point angle [°]	138	
Material - Coating	Solid Carbide – AlTiN-Si	
Tests (i)		
Cutting conditions	f [mm/rev]	v_c [m/min]
	0.15	150
Position	Range of postures C [°]	
1	-5 to 115	
2	15 to 165	
3	-30 to 100	
4	-5 to 115	
Tests (ii)		
Cutting conditions	f [mm/rev]	v_c [m/min]
	0.05 - 0.15 - 0.25	50 - 150 - 250
Position	Posture C [°]	
2	15	

To analyse how drilling position affects hole quality, four distinct positions along the front axis of the robot's work range were tested (Fig. 2(a)). All discussions will be carried out with respect to the *Oxyz* coordinate system, representing the TCP (Tool Centre Point). The 6-axis robot provided an additional degree of freedom, allowing definition of an angle C at the TCP, which specifies available postures for each position (see some examples of the range of postures for position 2 in Fig. 2(b)). These postures, characterized for all four positions, are listed in Table 1. In total, 16 postures were tested for each of the four positions, resulting in 64 drilling configurations, with each test repeated three times.

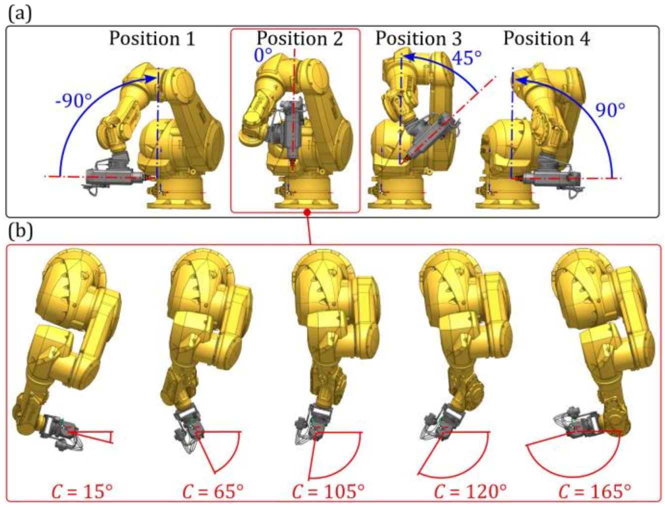

Figure 2. Robotic drilling: range of positions (a) and examples of postures for position 2 (b)

2.2. Hole defect analysis

The use of 6-axis robots for metallic drilling introduces eccentricity defects, $\vec{\Delta}$, mainly at the hole entry due to insufficient robotic rigidity [3] (Fig. 3(a)). These defects are induced by an in-plane *xy* displacement of the original drilling axis during the drilling phase, leading to quality defects and positional error, which could both be independently corrected. Understanding these defects is essential for developing compensation strategies. Fig. 3(b) illustrates the phases of robotic compliance leading to poor hole quality, while Fig. 3(c) depicts the force evolution throughout these phases.

Phase **I**: As the drill penetrates the material, the axial thrust force increases. Due to the robot's low rigidity, this induces a displacement $\vec{\Delta}$ in the *xy*-plane (mainly due to static deflection), directly proportional to the cross-compliance terms C_{zx} and C_{zy} [mm/N] (i.e. effect of the deformation of the robot in the x and y directions, respectively, according to a force applied in the z direction). These cross-compliances vary with robot position and posture. Consequently, the drilling position shifts with the thrust force.

Phase **II**: Once the drill is fully immersed, the axial thrust force stabilizes, causing deflection $\vec{\Delta}$ to remain constant and inducing a quasi-static in-plane deviation trough the phase. The drilling then proceeds in a straight line, parallel to the initial drilling axis.

Phase **III**: This stage is critical for generating drilling defects. As the drill exits the hole, the axial thrust force decreases, reducing static deflection to zero ($\vec{\Delta}$). The drill axis returns to its initial position, pushing the tool towards the opposite hole wall. In-plane forces $\vec{F_x}$ and $\vec{F_y}$ (Fig. 3(c)) increase.

Phase **IV**: During tool retraction, the compressed tool scrapes the hole wall, creating typical eccentricity defects in robotic drilling. This affects the hole geometry (roundness, cylindricity, and nominal diameter), surface integrity, and makes the holes unusable in fields such as aerospace.

This phenomenological observation allows for the inclusion of a defect compensation step directly counteracting the displacement $\vec{\Delta}$ induced by static deflection between Phases III and IV.

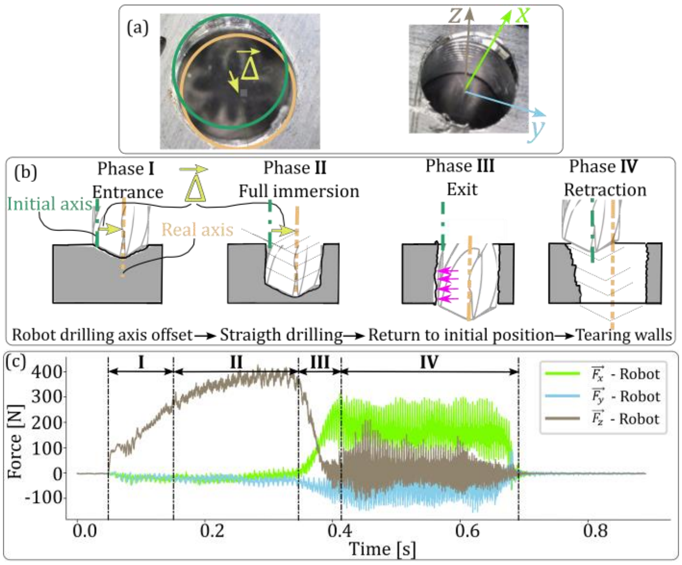

Figure 3. Hole defect analysis: defects (a), phases (b) and cutting forces (c)

2.3. Systematic method for improving hole quality

Based on these previous observations, a five-step methodology was developed to reduce defects through posture optimization and static deflection compensation, as described below:

1. Defining the spatial drilling position (Fig 2(a)): The first step involves determining the spatial position of the hole relative to the robot, typically constrained by spatial arrangement, accessibility, and setup considerations for the workpiece.
2. Posture evaluation: Once the hole position is determined, preliminary drilling tests are conducted to evaluate a range of postures for a given position. Since cross-compliance may vary by a factor of two to three depending on the robot's posture [7], it is crucial to assess their effect on hole quality. A series of drilling operations is carried out within the feasible postures range for the chosen position.
3. Optimal posture selection using the hole defect criterion D: From the results, the optimal posture is selected using the hole defect criterion D proposed in eq. (1).

$$D = \frac{(\rho_e c_e + \rho_m c_m + \rho_s c_s)}{\varphi_i} h + \tan(\theta_{\text{off}})\, h + \frac{(\rho_e \varphi_e + \rho_m \varphi_m + \rho_s \varphi_s) - \varphi_i}{\varphi_i} h \quad (1)$$

Where,

- c_e, c_m and c_s [mm]: circularity at the entry, middle, and exit of the hole, respectively.
- φ_e, φ_m, φ_s [mm]: hole diameters at the entry, middle, and exit, respectively.
- φ_i [mm]: nominal hole diameter.
- θ_{off} [°]: offset angle defined as the deviation between the axis of the best-fit cylinder obtained by least squares and the ideal axis.
- h [mm]: nominal thickness of the drilled material.
- ρ_e, ρ_m and ρ_s: weights assigned at the entry, middle, and exit of the hole, respectively. This criterion highlights major robotic drilling defects: diameter deviations, circularity issues, and axis offsets angles [3]. Weights (ρ_e=0.6, ρ_m=0.2, ρ_s=0.2) were assigned based on observed defects, emphasizing entry-related issues during the robotic drilling of aluminium. It is important to note that the choice of the latter facilitates the highlighting of the effects of robotic defects but does not influence the qualitative evolution of the results and the associated conclusions.

As the arithmetic roughness and the cylindricity do not influence the qualitative evolution of the defect criterion D, they were not included in it. The three terms in the D criterion respectively account for circularity error, off-axis angle, and measured vs nominal diameter, each measured at three levels. To ensure comparability and limit setup-related influences (e.g., material thickness, tool diameter), the first and third terms are weighted by the ratio of thickness to nominal tool diameter.

4. Determining displacements: After identifying the optimal posture, a two-step compensation strategy is applied. The first step determines the displacement amplitude $|\vec{\Delta}|$ [mm] (Fig. 3(b)), representing the offset between the actual drilling axis and the initial tool axis at the entry point, reflecting the robot's static deflection during drilling. This is measured with a digital microscope. The second step calculates the components $|\Delta_x|$ and $|\Delta_y|$ of the displacement based on the in-plane forces $\vec{F_x}$ and $\vec{F_y}$ and the in-plane resultant force $\vec{F_{res}} = \vec{F_x} + \vec{F_y}$, using eq. (2) and (3):

$$|\Delta_x| = |\vec{\Delta}| \frac{|\vec{F_x}|}{|\vec{F_{res}}|} \quad (2)$$

$$|\Delta_y| = |\vec{\Delta}| \frac{|\vec{F_y}|}{|\vec{F_{res}}|} \quad (3)$$

5. Defect compensation: Once the displacements are determined, the final step is to implement a compensation phase for the computed $|\Delta_x|$ and $|\Delta_y|$ at the end of drilling (between Phase III and Phase IV in Fig. 3(b)). This phase involves stopping the drill rotation and moving it at a low feed rate (f = 0.00125 mm/rev) to minimize dynamic effects along the delta direction $\vec{\Delta}$ .This adjustment enables the relaxation of the in-plane forces $\vec{F_x}$ and $\vec{F_y}$.

3. Results and discussions

3.1. Robotic posture and position influence on hole quality

Fig. 4 proves the direct influence of the posture on the hole quality index at the four previously defined drilling positions under the nominal cutting conditions (v_c=150 m/min and f=0.15 mm/rev). Based on eq. (1), the aeronautic standards [4] correspond to a threshold D of 0.13 mm; this benchmark was used to evaluate the drilled holes.

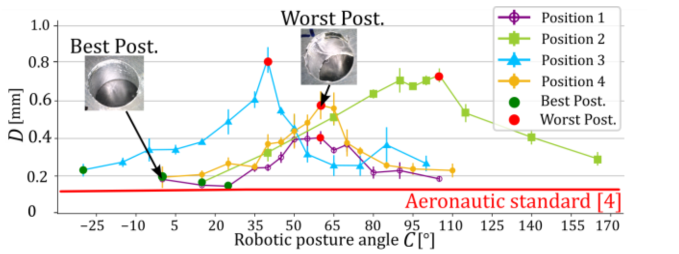

Figure 4. Influence of the robotic posture on hole quality (v_c=150 m/min, f= 0.15 mm/rev).

The defect index curves based on posture follow a bell-shaped trend (Fig. 4), consistent with robotic compliance curves relative to posture as reported in the literature [8]. This behaviour was observed across all tested positions, supporting the statement that hole quality directly depends on the robot's static deflection, rigidity, and compliance. Optimal postures were identified and highlighted with green marks. These optimal postures were C=25°, C=15°, C=−30° and C=0° for positions 1, 2, 3, and 4, respectively. On the other hand, worst postures identified with red marks were C=60°, C=105°, C=40° and C=60° for positions 1, 2, 3, and 4, respectively. A two to fourfold difference in defect index was observed between the best and worst postures for a given position, emphasizing the critical need for posture optimization to ensure acceptable hole quality, as illustrated by the associated hole images. The overall best results are highlighted in Fig. 4 and are obtained with position 1 and posture C=25°.

3.2. Defect compensation

After identifying the optimal posture for each position, displacements $|\vec{\Delta}|$ of approximately 0.7 mm were measured at all four positions. The compensation strategies were then evaluated and the resulting hole quality is presented in Fig. 5 for the optimal and the worst identified postures for each position. Holes drilled with unfavourable postures showed poor quality, with defect indices exceeding aerospace standards by a factor of six. Fig. 5 shows defect indices *D* reached 0.5–0.6 mm. These indices correspond to diameter and circularity deviations in the entry zones ranging from 0.2 to 0.5 mm. The application of compensation strategies reduced defects by a factor of two. When combined with posture optimization, these strategies met aerospace requirements, achieving defect indices below 0.13 mm and reducing diameter and circularity deviations to approximately 0.05 mm. The proposed method reduced the hole defect index from 0.5 mm to 0.1 mm—a fivefold improvement—and minimized static deflections ($\vec{\Delta}$) from 0.7 mm to near-zero. These results show that addressing static deflection alone enables a compensation strategy that significantly improves hole quality, independently of dynamic and thermal effects [10].

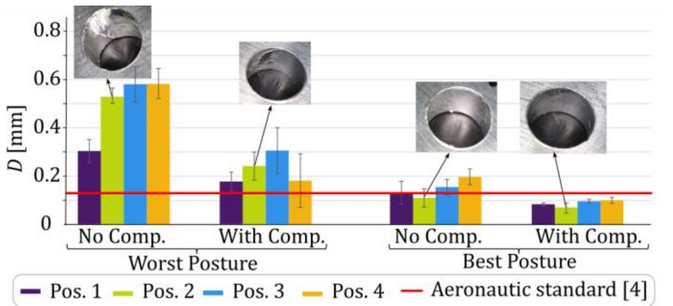

Figure 5. Effect of the defect compensation on the hole quality (v_c=150 m/min, *f*= 0.15 mm/rev).

3.3. Effect of cutting conditions and CNC comparisons

The impact of cutting speed and feed rate variations was evaluated through additional drilling tests on both robotic system and a CNC machine, allowing for a comparison of hole quality under high rigid system. Robotic cross compliance was measured at 2 µm/N, while CNC compliance was 0.02 µm/N.

Fig. 6(a) compares robotic cutting forces (with compensation, with position 2 and *C*=15°) to those obtained without using compensation. As expected, robotic forces showed increased in-plane components ($\vec{F_x}$ and $\vec{F_y}$) at the end of drilling. Implementing defect compensation to relax these forces proved essential for producing high-quality holes.

Fig. 6(b) summarizes the comparative hole quality results. Cutting forces are particularly sensitive to the feed rate, which explains the linear increase in hole defects with higher feed rates. However, they exhibit minimal sensitivity to cutting speed, which accounts for the lack of correlation between hole quality and cutting speed (whether increasing or decreasing). Indeed, increasing cutting speed from v_c=50 m/min to v_c=150 m/min improves hole quality, but further increasing it to v_c=250 min/min generates dynamic effects that significantly degrade hole quality and reduce repeatability. This results from nonlinear interactions between cutting conditions, tool characteristics, tool holder, and robot posture. These findings emphasize the importance of selecting appropriate cutting conditions.

With an average index *D*=0.045 mm, CNC-drilled holes exhibited defect indices roughly half those of robotically drilled holes even with defect compensation. For robotic drilling, defect indices averaged at 0.1 mm, with hole diameter and cylindricity deviations around 0.03 mm This performance is noteworthy, considering the CNC machine is 100 times stiffer than the robotic system, yet the defect index only doubles while consistently meeting industrial standards. Although the addition of an extra phase increases cycle time by approximately 2 seconds, the compensation method combined with posture optimization effectively reduced defects by up to a factor of two under the tested conditions, achieving holes that met the required aeronautical standard in most (seven out of nine)of the analysed cutting conditions.

Finally, profilometer measurements of arithmetic roughness *Ra* confirm visual observations and emphasize the advantages of compensation in robotic drilling (Fig. 6(b)). The *Ra* values improved significantly, decreasing from 3.2 µm for holes drilled without compensation to less than 1.6 µm with compensation, approaching the values reported by CNC machines (0.8 µm).

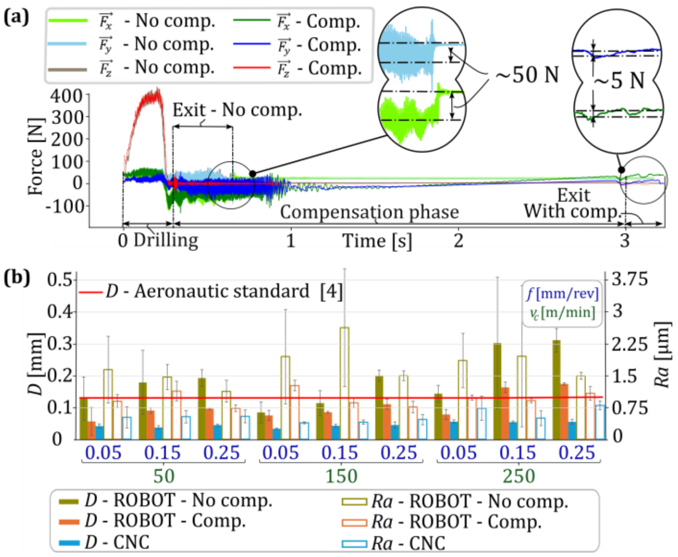

Figure 6. Drilling forces during compensation (v_c=150 m/min, *f*=0.15 mm/rev) (a) and hole defect index diagram as a function of the change of cutting conditions (b)

4. Conclusions

This study demonstrates that robotic posture optimization and defect compensation significantly enhance quality in robotic drilling, achieving aeronautic industry standards. By analysing the effects of compliance and rigidity on defects, a systematic methodology was developed to identify optimal postures and apply compensation strategies, reducing diameter deviations, circularity defects, and axial misalignments. The proposed method reduced the proposed hole defect index by a factor of five.

Additionally, arithmetic roughness (*Ra*) improved from 3.2 µm to 1.6 µm with the robot. Despite the robot's lower rigidity than CNC machines (100 times), the optimized methodology consistently met industrial standards. Sensitivity to cutting parameters highlights the importance of minimizing thrust force to reduce its impact on static deflection.

This research provides a framework to address robotic compliance challenges in drilling, supporting the broader adoption of 6-axis robots for high-precision machining. From an industrial perspective, this highlights the potential use of 6-axis robots for drilling large, complex metallic parts in small and medium batches. This approach eliminates the need for hardware systems that currently restrict 6-axis robots to merely positioning actuators, also limiting their use to unique drilling operations.

Acknowledgments

The authors would like to acknowledge funding the project MachStack via conventions 1910097 (Région Wallonne), and ZL-2021/00273 (Hazitek program).

References

[1] Verl A, Valente A, Melkote S, Brecher C, Ozturk E, Tunc LT. Robots in machining. CIRP Annals. 2019;68(2):799-822.

[2] Swan R, Penney J, Corson G, Nazario J, Schmitz T. Surface location error in robotic milling: Effect of combined low frequency and high frequency vibration modes.CIRP Journal of Manufacturing Science and Technology 49 (2024) 203-215.

[3] Beuscart T, Arrazola PJ, Tinel N, Ducobu F. Effect of Cutting Conditions on Surface Integrity when Robotic Drilling of Aluminum 6082-GFRP Stacks. Procedia CIRP. 2024;

[4] Devlieg R. High-Accuracy Robotic Drilling/Milling of 737 Inboard Flaps. SAE Int J Aerosp. 18 oct 2011;4(2):1373-9.

[5] Pilny L, De Chiffre L, Piska M, Villumsen M, Hole quality and burr reduction in drilling aluminium sheets. CIRP Journal of Manufacturing Science and Technology 5 (2012) 102-107.

[6] Liang J, Bi S. Design and experimental study of an end effector for robotic drilling. Int J Adv Manuf Technol. sept 2010;50(1-4):399-407.

[7] Dong S, Meng D, Zheng K, Liao W. Experimental study on robotic rotary ultrasonic drilling of CFRP/aluminum stacks. J Phys: Conf Ser. 1 juin 2021;1887(1):012013.

[8] Bu Y, Liao W, Tian W, Zhang J, Zhang L. Stiffness analysis and optimization in robotic drilling application. Precision Engineering. juill 2017;49:388-400.

[9] Lee JH, Kim SH, Min BK. Posture optimization in robotic drilling using a deformation energy model. Robotics and Computer-Integrated Manufacturing. déc 2022;78:102395.

[10] Heisel U, Richter F, Wurst K.-H, Thermal Behaviour of Industrial Robots and Possibilities for Error Compensation. CIRP Annals.1997;46(1):283-286 .

[11] Chen D, Yuan P, Wang T, Cai Y, Xue L. A Compensation Method for Enhancing Aviation Drilling Robot Accuracy Based on Co-Kriging. Int J Precis Eng Manuf. août 2018;19(8):1133-42.